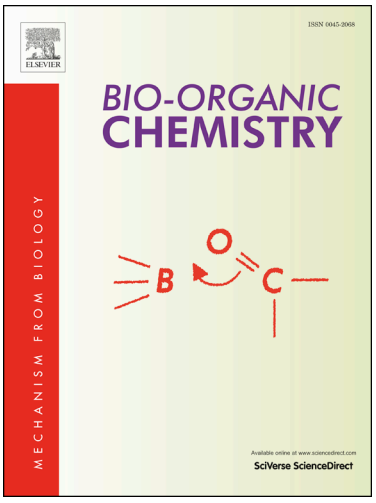

Benzimidazole scaffold based hybrid molecules for various inflammatory targets: Synthesis and Evaluation

Gaganpreet Kaur, Om Silakari

PII: S0045-2068(18)30215-3
DOI: https://doi.org/10.1016/j.bioorg.2018.05.014
Reference: YBIOO 2367

To appear in: *Bioorganic Chemistry*

Received Date: 5 March 2018
Revised Date: 16 May 2018
Accepted Date: 16 May 2018

Please cite this article as: G. Kaur, O. Silakari, Benzimidazole scaffold based hybrid molecules for various inflammatory targets: Synthesis and Evaluation, *Bioorganic Chemistry* (2018), doi: https://doi.org/10.1016/j.bioorg.2018.05.014

Benzimidazole scaffold based hybrid molecules for various inflammatory targets: Synthesis and Evaluation.

Gaganpreet Kaur and Om Silakari*

*Corresponding Author- Molecular Modeling Lab (MML), Department of Pharmaceutical Sciences and Drug Research, Punjabi University, Patiala. Punjab 147002, India.

E-mail: omsilakari@gmail.com, Telephone: +919501542696

ABSTRACT

Designing of hybrid drugs with specific multitarget profile is a promising line of attack against inflammation. In light of this, a series of benzimidazole scaffold based hybrid molecules were designed by integrating benzimidazoles (containing pharmacophoric elements for COXs and LOXs inhibitors) with phthalimide subunit of thalidomide (pharmacophore element for TNF-α inhibitor) under one construct via molecular hybridization strategy. The designed molecules were synthesized and evaluated for their inhibitory activity against COXs (COX-1, COX-2), LOXs (5-LOX, 15-LOX) enzymes as well as TNF-α inhibitory effect. The results revealed that, compounds (**3a-l**) obtained showed inhibition in submicromolar range against COXs and LOXs targets whereas milder inhibitory activity was obtained against lipopolysaccharides (LPS)-induced TNF-α secretion by murine macrophage-like cells (RAW264.7). Within this class of compounds, **3j** emerged as having alluring multiple inhibitory effects on set of COX-1/2 and 5-/15-LOX enzymes (COX-1 IC_{50}=9.85μM; COX-2 IC_{50}=1.00μM; SI=9.85; 5-LOX IC_{50}=0.32μM; 15-LOX IC_{50}=1.02μM) in conjunction with a good anti-inflammatory and analgesic activities. Additionally, compound **3j** showed gastrointestinal safety with reduced lipid peroxidation. Docking results of compound **3j** with COX-2 and 5-LOX were also consistent with the *in vivo* anti-inflammatory results.

Keywords: Anti-inflammatory, Benzimidazole scaffold, COXs, Hybrid drugs, LOXs, Multitarget profile, TNF-α

1. Introduction

Despite years of studies and irrespective of long passage of anti-inflammatory drugs, efficacy and safety of the drugs- a set of extremely important fundamental issues remains unresolved [1]. The growing realization that inflammation is a complex, multifactorial and crucial in many diseases opens up a whole new avenues for treatment [2]. Current research emphasizes designing of hybrid drugs with a specific multi-target profile as the promising line of attack against inflammation [3].

Demand for hybrid drugs has driven the pursuit of structures possessing multitargeted aptitude. It is well documented that designing of novel drugs on "privileged scaffold" is one of the successful directions in drug discovery. "Privileged scaffold" offered an optimal source of core structure and presented remarkable capability of binding across multitudes of therapeutically relevant biological targets [4]. Among the privileged scaffolds engaged in drug designing, focus on benzimidozole nucleus is noteworthy. Above and beyond synthetic versatility, benzimidazole scaffold endows its derivatives with diverse portfolio as of inflammation targeted drugs by virtue of its inherent affinity against various inflammation related targets. This inspiring biological background has raised lots of concerns on their suitability as a viable scaffold for design of multitargeted anti-inflammatories [5]. On the other hand thalidomide is another significant drug molecule noticeable for its well-known inherent TNFα-inhibitor property liable for its distinguishing immunomodulatory and anti-inflammatory properties. Structure activity studies, analogs and metabolites of thalidomide now clearly disclosed that phthalimide subunit (pharmacophore) of thalidomide is essential for its distinctive pharmacological functions whereas its glutarimide portion (toxicophore) facilitates binding to the human cereblon gene (component of an E3 ubiquitin ligase

complex), which is a primary target protein responsible for thalidomide-mediated teratogenicity [3,6].

Following the emerging trend of hybrid drugs and encouraged by biological background of benzimidazole and thalidomide, the possibility of designing novel hybrid molecules was therefore explored using privileged benzimidazole as a core scaffold, which combines, under one construct, pharmacophoric elements that characterize well-known classes of inhibitors of cyclooxygenase isoenzymes (COXs), lipoxygenase isoenzymes (LOXs) and tumor necrosis factor-alpha (TNF-α) via molecular hybridization drug design strategy. A preview of the overall design strategy illustrated in Figure 1. The pharmacophoric element needed for cyclooxygenase and lipoxygenase inhibitors where they shares the same "privileged" benzimidazole scaffold as putative binding motif integrated with phthalimide subunit of thalidomide as pharmacophoric group for TNF-α inhibition. It was envisaged that such a benzimidazole scaffold based hybrid molecules might therefore, endowed with an efficient and safer anti-inflammatory action.

The relevant set of targets selected in this study, cyclooxygenases (COX- 1, COX-2), TNF-α, and lipoxygenases (5-LOX, 15-LOX) were chosen for variety of reason. The first and foremost, is all of them shares inflammation as the therapeutic niche. Secondly, cross-talks (or communications) amongst inflammatory pathways may lead to strong pharmacodynamics synergy between the elected targets. COXs and TNF-α were carefully selected set of primary targets. The COXs are the principally involved and overly explored best known targets of anti-inflammatory drugs to date [7], while TNF-α is a central key player in the initiation of multiple inflammatory cascades [8]. Moreover because of suggested role of lipoxygenase in the mechanism and safety of anti-inflammatory drugs [9] they are intentionally being elected as key inflammatory target for the present study.

2. Results and discussion

2.1 *Design rationale*

The scientific rationale behind the design concept is the "synergistic benefit" that could be achieved when COXs and LOXs inhibitory activities combined with the inhibition of TNF-α in alleviating inflammation. Support for this concept provided by findings evolving around the use of NSAIDs and COX-2 selective inhibitors. First is, NSAIDs and coxibs preferentially decreased prostaglandin (PG) compared with thromboxane (TX) synthesis, and this imbalance may create a persistent "rebound effect" on the proinflammatory signaling hence increases the TNF-alpha production, an effect that is paradoxical and certainly undesired for anti-inflammatory drugs [10]. Second is, selective inhibition of cyclooxygenase (COX) pathway may also lead to a shunt of the arachidonic metabolism towards the other untargeted lipoxygenase (LOX) pathway thus increasing the formation of proinflammatory and gastrotoxic leukotriene's [11].

A possible reason of these effects is redundancy and robustness in many biological networks and pathways in which cells often find way to compensate for protein whose activity is affected by a drug [12]. Moreover an ideal drug may be one whose efficacy is based not on inhibition of a single target but rather on rebalancing of several proteins or events that contributed to etiology, pathogenesis and progression of diseases. The described effects support the need for paradigm shift in drug discovery from single disease target inhibitor towards multi-target concept, which might favors improved safety and efficacy. It is therefore seems reasonable that a balanced approach targeting selective inhibition of COX-2 combined with inhibition of LOXs and TNF-α could deliver superior therapeutic benefits in treatment of inflammation. As of yet no such hybrid molecules holding anti-inflammatory profile indicated in the literature.

2.2 *Chemistry*

The synthetic pathway for the target hybrid compounds is illustrated in Scheme 1(A). Scheme 1(A) describes the facile cyclisation reaction of 4-nitrobenzene-1,2-diamine with cyanogen bromide in water to give desired 5-nitro-1*H*-benzimidazol-2-amine scaffold **1** [13], which was transformed into corresponding 2-(5-nitro-1*H*-benzimidazol-2-yl)-1*H*-isoindole-1,3(2*H*)-dione an intermediate hybridized structure **2** by means of phthaloylation reaction using *o*-phthaloyl dichloride in the presence of pyridine [14]. The synthesis of target hybrid molecules was achieved by cross coupling reactions. Among the available synthetic approaches, we opted to begin with the N-arylation reactions driven by potassium carbonate/*N*,*N*-dimethyformamide system *in situ* which led to the coupling of free (NH) site in benzimidazole scaffold of intermediate hybridized structure **2** with different aryl halides as their electrophilic coupling partner leading to formation of target hybrid compounds (**3a-l)** [15]. Approximate presentation of what may happen depicted in Scheme 1(B). In Scheme 1(B), reaction (I) is deprotonation which involves generation of anionic nucleophile by reaction of sodium carbonate and free (NH) site of benzimidazole in *N*,*N*-dimethylformamide as solvent. In order to balance charge, the *in situ* generated anionic nucleophile further interact with floating potassium ion and converted into the corresponding potassium salts. While reaction (II) is expected to be classic S_N2 substitution in Scheme 2.

2.3 *Biological evaluation*

2.3.1 *In vitro COX-1 and COX-2 inhibitory assay*

Target compounds **3a-l** were tested for COX-1 and COX-2 inhibition at five concentrations (0.01, 0.1, 1, 10 and100μM) to determine the concentration produced 50% inhibition of COX-1 and COX-2 enzymes (IC_{50} values) and their selectivity indices (SI= IC_{50}COX-1/ IC_{50}COX-2) using indomethacin and celecoxib as reference drugs. The results recorded in Table 1 indicated that these compounds exhibit broad range of COX-1/2 activities (COX-2 IC_{50}=1.0 to >100μM range; COX-1 IC_{50}=7.0 to >100μM range). Since both isoforms (COX-1

and COX-2) are structurally quite similar (>50% sequence homology) their three-dimensional structures are almost superimposable and they also share common binding partner(substrate), accordingly results further explicitly indicated that some compounds are more active on COX-1 and others are on COX-2. Among them, methoxy, phenethyl, isopropyl, and nitro substituted compounds (**3b, 3f, 3h, and 3k**) provided much weaker COX inhibition (COX-1 IC_{50}= >15μM; COX-2 IC_{50}= >100μM). However for the methyl substituted compounds, COX-2 potency order was **3d** > **3e** >**3c**, it appeared that *m*- position of the methyl (**3d**) at peripheral phenyl group were more favourable than *o*- and *p*- positions. Compound **3c**, which provided a potent COX-1 inhibition (COX-1 IC_{50}= 7.76μM) among series, on the other hand did not inhibit COX-2 at concentration of 10μM. Comparison of **3h** (COX-1 IC_{50}= 17μM; COX-2 IC_{50}=>100μM) with that of **3i** (COX-1 IC_{50}= 15.99μM; COX-2 IC_{50}=16.07μM) revealed that presence of *p*-position of *tert*-butyl group provided an optimal combination of *in vitro* COX-1/COX-2 inhibitory effects hence seems to be more favourable than isopropyl group. Compounds **3j** displayed significant COX-2 inhibitory activity (COX-2 IC_{50} = 1.00 μM; COX-1 IC_{50} = 9.85 μM), and it was 4-fold more potent compared to reference drug indomethacin (COX-2 IC_{50} = 4.02 μM) although less potent than celecoxib (COX-2 IC_{50} = 0.04 μM). It appeared that introduction of phenyl substituent at the *m*-position of peripheral phenyl ring (**3j**) was most favourable for the cyclooxygenase inhibition. It is notable that substituting a phenylethyl group (**3f**) for a 3-phenylbenzyl (**3j**) resulted lesser potent inhibitor of COX-2(IC_{50}=29.73 μM). In terms of selectivity index (SI), compound **3j** showed modest COX-2 selectivity (SI=9.85) than the reference drug celecoxib although put on show good selectivity when compared to its structural analogue indomethacin, an indole based NSAIDs (SI=0.08) as shown in Table 1.

2.3.2 *In vitro 5-LOX and 15-LOX inhibitory assay*

Target compounds **3a-l** were tested for human 5-LOX and 15-LOX inhibition at five concentrations (0.01, 0.1, 1, 10 and 100µM) to determine the concentration produced 50% inhibition of 5-LOX and 15-LOX enzymes (IC_{50} values) using reductive inhibitor nordihydroguiarectic acid (NDGA) as reference drug. The results reported in Table 1 indicated that all the target compounds had more potential in inhibitory human 5-LOX (IC_{50} value range from 0.32µM to >5µM) compared to 15-LOX (IC_{50} value range from 1.02 to >5µM). The 5-LOX inhibitory potency was of the order **3j > 3a > 3e >3b >3h > 3d > 3k > 3f >3l >3g >3c> 3i**.Within subgroup of methoxy substituted compounds lipoxygenase potency order was **3a**>**3b**. Incorporation of isopropyl group (**3g**) resulted in potent 15-LOX inhibition (15-LOX IC_{50}= 1.76 µM) although it was less potent than reference drug NDGA. As indicated, compound **3j** possessed the most potent LOX inhibitory activity and the moderate subtype selectivity for 5-LOX (3-fold selectivity versus 15-LOX). Compound **3j** was 1.5 fold more potent inhibitor of 5-LOX than the reference drug NDGA (5-LOX IC_{50}= 0.52µM). It appeared that presence of the biphenyl ring (**3j**) was most favourable for the dual 5/15-lipoxygenase inhibition. Also compounds **3h** and **3j** (15-LOX IC_{50}= 1.05 µM and 1.02 µM respectively) were found to be slightly more potent than that of NDGA (15-LOX IC_{50}=1.10µM) suggesting that these compounds could act as antioxidants. Additionally, compound **3j** exhibited significant dual COX/LOX inhibition over the reference drugs.

2.3.3 *In vitro TNF-α inhibitory assay*

Target compounds **3a-l** were tested against LPS-induced TNF-α secretion in mouse RAW264.7 macrophages at different concentrations to determine the concentration produced 50% inhibition of TNF-alpha (IC_{50} values) using dexamethasone as reference drug. The results of biological activity of all target compound have been presented in Table **1.** It was observed that a majority of the target compounds of this series demonstrated weak inhibitory activities as compared to the standard dexamethasone while few of them (**3f**, **3g**) found to

inactive even at higher tested concentration(>500 μM). However, single compound **3j** among the series, in particular**,** showed IC_{50} value of 461μM against TNF-alpha inhibitory activity.

2.3.4 In vivo assay

2.3.4.1 Carragennan-induced paw edema model

Carrageenan test is greatly sensitive to clinically useful steroidal and nonsteroidal anti-inflammatory drugs and has been widely accepted as a useful model to measure anti-inflammatory drugs. Carrageenan injection generated intense inflammation (edema as being the principal symptom) which peaked between 3-5 hours and is attributed to release of inflammation related mediators (e.g. prostaglandins, leukotrienes, cytokines and nitric oxide), which is the moment when its maximum effect is demonstrated and the moment when the anti-inflammatory effect of the test product is best observed. The pharmacological results listed in Table 2(see also Table 2S, supplementary data for detail) and illustrated in Fig. 2 represents the mean changes in paw edema volume mL±SD of animals pretreated with the reference drugs and test compound **3j** after 3h and 5h from the induction of inflammation, together with the percent inhibition of induced rat paw edema by the test compound (percent anti-inflammatory activity). Statistical differences of control, reference and test groups were carried out using F test (ANOVA) followed by post hoc test. The screened results revealed that, the strong inhibition of edema was observed after 3 h. The tested compound **3j** showed significant anti-inflammatory activity (% edema reduction=81.88) comparable to that of celecoxib (87.59% edema reduction) whereas higher than indomethacin (79.41% edema reduction). The significant inhibition of edema of **3j** coupled with its marked *in vitro* inhibitory effects against cyclooxygenases, lipoxygenases and TNF-α suggested an obvious mechanism of anti-inflammatory action.

2.3.4.2 Analgesic activity

Sodium chloride-induced writhings was significantly reduced in rats receiving the test compound **3j,** indicating peripheral analgesic effect. The analgesic activity of the compounds was done at the same dose as used for anti-inflammatory activity. The positive controls, indomethacin and celecoxib, inhibited the writhing response by 76.28% and 78.57% respectively whereas the analgesic effect of **3j** was 77.14% at 3hr post drug administration (Table 3).

2.3.4.3 Gastric ulcerogenic activity

The compound (**3j**), which was screened for analgesic activity, further screened for their acute ulcerogenic risk. In the indomethacin induced ulcerated control group, the severity index was 5.33±0.47 which was significantly reduced by the newly synthesized compound **3j** as shown in Table 3. Compound **3j** showed severity index of 1.16, which is less than one-fourth of the value of indomethacin hints at that compound **3j** is relatively selective for COX-2.

2.3.4.4 Lipid peroxidation

Compound **3j** showing significantly reduced gastric mucosal lesions is also reported to show reduced gastric MDA content, an index of lipid peroxidation-mediated tissue damage. Therefore, by determining the MDA content it can be make certain that the compound is actually lesser toxic to gastric mucosa. The lipid peroxidation was measured as nmoles of MDA/100mg of tissue. Animals treated with indomethacin exhibited 2.89, whereas control group showed 1.09 and the groups treated with synthesized compounds showed lipid peroxidation content of 1.17(Table 3), suggesting that newly synthesized compound **3j** results in relatively lesser gastric mucosal injury.

2.4 Structure-activity correlation

Careful inspection of structures of the tested compounds revealed that central core (benzimidazole scaffold) might contribute largely to the interaction with the amino acid

residues of the enzyme's active site and is mainly responsible for projecting the pharmacophoric elements in correct orientation for the efficient binding. In general substantial part of the compounds obtained showed dual inhibition of both COX-1/2 and 5/15-LOX enzymes whereas weak inhibitory activity was obtained against LPS-induced TNF-α secretion. The *in vitro* data acquired for this class of compounds further indicated that COX and LOX inhibition can be manipulated by varying the substituents attached at N-1 position (D framework, see Fig.1) of target compounds but virtually on the TNF-α inhibitory activity no significant impact was observed. It is also notable that replacement of benzyl group in the D framework of the target compound (see Fig. 1 and Table 1) by phenylethyl group as represented by **3f** provided weak COX-2 inhibition and moderate COX-2 selectivity (COX-2 IC_{50}=29.73μM; SI=15.2) while retaining 5- and 15-LOX inhibitory activity and led to complete loss in TNF-α inhibitory activity. Individual compound **3j** showed significant dual COX/LOX inhibition (COX-1 IC_{50}=9.85μM, COX-2 IC_{50}=1.00μM; SI=9.85; 5-LOX IC_{50} = 0.32 μM; 15-LOX IC_{50} = 1.02 μM) along with milder TNF-α inhibitory activity for which the presence of 3-phenylbenzyl group at the N-1 position, electron withdrawing group i.e. nitro substituent at C-5 position of benzimidazole scaffold observed to be beneficial features clearly.

2.5 Anti-inflammatory docking study

All the designed compounds were docked into the active sites of COX-1, COX-2, 5-LOX and 15-LOX. Results of molecular docking analysis indicate that all the designed and subsequently synthesized compounds especially **3j**, were having equally good binding affinity towards COX-2, 5-LOX and 15-LOX, while **3c** showed significant binding affinity in COX-1. The binding energy of docked compounds towards COX-2 was found to be between −24.56 and −31.94 kcal/mol, in COX-1, it ranged from −20.73 and −47.99 kcal/mol, in 5-LOX, the binding energy ranged between −52.96 and −56.77 kcal/mol and in 15-LOX, it was

found between -25.63 and 57.68 kcal/mol. The most potent compound **3j** revealed by biological evaluation showed good binding energy among the docked compounds with the score of −31.94 kcal/mol towards COX-2, −56.77 kcal/mol towards 5-LOX and 57.68 kcal/mol towards 15-LOX. This binding energy score reflects the affinity of **3j** towards both COX-2 and 5-LOX. While the most potent compound against COX-1, **3c** showed good binding energy among the docked compounds with the score of −44.02 kcal/mol towards COX-1

Analysis of docked complex of **3j** and COX-2 proved that the nitro group of **3j** plays a crucial role in COX-2 inhibition by interacting with both Phe-518 and Arg-513 (Fig. 3). Following the designing of the molecules, the biphenyl rings formed π-π interactions with Tyr-355 and Arg-120, respectively. While, analysis of docked complex of **3j** and 5-LOX showed significance of nitro group for 5-LOX inhibition also. The nitro group formed interactions with His-432 present in the active site of 5-LOX. Moreover, nitrogen of benzimidazole nucleus forms hydrogen bonding with Gln-557. Complying with the π-π interactions in COX-2, in 5-LOX also biphenyls formed π-π interaction with His-600 and an additional π-π interaction formed between benzimidazole ring and His-367(Fig. 4). Similarly, analysis of docked complex of **3j** and 15-LOX showed several π-π interactions between fused aryl ring of benzimidazole and Val-348, and between aryl ring of thalidomide and Val-116. Additionally, the nitro group formed another π-π interactions with Tyr-348 present in the active site of 15-LOX (Fig. 5). Finally, most significant COX-1 inhibitor, **3c** showed hydrogen bond between N of benzimidazole and Ser-510 (Fig. 6). Additionally, another hydrogen bond interaction was observed between nitro group and Ile857. While the thalidomide ring formed the hydrophobic interactions with the catalytic domain to improve the overall binding affinity.

3. *Conclusion*

The present study shows that the synthesized benzimidazole scaffold based hybrids represents promising multitargeting potential by influencing various inflammation-related targets. E.g., COX-1, COX-2, 5-LOX, 15-LOX and TNF-α. Compound **3j** showed potent dual inhibition of both COX-2 and 5-LOX enzymes was also screened for its *in vivo* anti-inflammatory activity, analgesic (algesia being the main symptom of inflammation) and ulcerogenic and lipid peroxidation activities. The results revealed that it showed significant decrease in carrageenan-induced paw edema in conjunction with good analgesic activity. Besides, compound **3j** offered gastrointestinal safety with reduced lipid peroxide profile. Biological results was also consistent with the docking studies in the active sites of the target enzymes (COX-2 and 5-LOX). Accordingly results of the study concluded that observed combination of COX-2 selectivity and 5-LOX inhibition in **3j** may be responsible for the efficient anti-inflammatory action and high gastrointestinal safety and thus supports the prevailing hypothesis.

4. Experimental section

4.1 Chemistry

All chemicals and solvents required for synthesis were procured commercially from various suppliers (Sigma, Merk and Loba) and were of LR grade, used without any purification. The solvents were dehydrated according to the standard methods. The synthesis was carried out using steam bath, magnetic stirrer and hot plate (Perfit), and solvents were recovered using rotary vacuum evaporator (Perfit). The completion of each reaction was monitored by thin layer chromatography (DC-Alufolien (20x20 cm) Kieselgel 60 F_{254} chromato plates) using hexane: ethylacetate (7:3 v/v) and chloroform: methanol (9.6:0.4 v/v) as a TLC development solvent system and visualized in UV chamber (Perfit) at short as well as long wavelengths. Impure compounds and intermediates were purified on silica columns from appropriate solvent. Compounds were purified by silica columns (100-200mesh) or recrystallization

technique. The melting point were recorded in open glass capillaries with electrical melting point apparatus and uncorrected. ^{1}H-NMR spectra were recorded on a Bruker Avance II 400 MHz NMR spectrometer using DMSO-d_6 (or in $CDCl_3$) as solvent and tetramethylsilane (TMS) as an internal standard. Proton chemical shifts are expressed in parts per million (ppm). ^{13}C NMR spectra were recorded on same spectrometer operating at 400 MHz. IR spectra were measured with Perkin Elmer RZX FT-IR and Bruker (Alpha E) FT-IR spectrometer. IR peaks were recorder at cm^{-1} scale. Mass spectra were recorded on Waters Q-TOF micro MS spectrometer at positive ionization mode (ESI+). The MS peaks were recorded as *m/z* ratio and corrected, using which candidate structures, their relative abundances were assessed.

Compounds **1**[13], **2** [14] and **3a-l** [15] were prepared according to reported procedures (see the Table 1S (Supplementary data) for the physicochemical properties and TLC data of compounds **3a-l**).

4.1.1. *Synthesis of 5-Nitro-1H-benzimidazol-2-amine (**1**)*

A suspension of 4-nitro-*o*-phenylenediamine (1.4g, 9.1mmol) in a solution of BrCN (0.97g, 9.2mmol) in water (30ml) was heated under reflux for 7hr, cooled and neutralized with 25% NH_4OH to pH 10-11. The formed precipitate was then filtered, washed with water, air-dried and recrystallized from hot water. The title compound was obtained as an oranges yellow shiny crystals. Yeild=1.28g (91.4%); mp. 245-247 $^{\circ}$C. ^{1}H-NMR (400 MHz, DMSO-d_6, δ ppm): 8.10 (d, 1H, *J*=2.2Hz, *ArH*), 7.90 (dd, 1H, *J* = 8.70, 2.2 Hz, *ArH*), 7.20 (d, 1H, *J* = 8.7 Hz, *ArH*), 6.90 (s, 2H, NH_2). ^{13}C-NMR (400 MHz, DMSO-d_6, δ ppm): 158.91, 139.92, 136.67, 116.50, 111.16, 106.16. IR (KBr, cm^{-1}): 3514, 3457 (N-H stretching), 3092 (C-H aromatic stretching), 1658(C=N ring stretching), 1587, 1507 (skeletal bands), 1421 (asymmetric N=O stretching), 1471 (N-H scissoring), 1336 (symmetric N=O stretching), 876

(N-H wagging). MS (+ESI-QTOF): m/z calculated for $C_7H_6N_4O_2$ $[M+H]^+$ 179.14, found 179.1(100%).

4.1.2. *Synthesis of 2-(5-Nitro-1H-benzo[d]imidazol-2-yl)isoindoline-1,3-dione (**2**)*

5-Nitro-1*H*-benzimidazole-2-amine (5.11g, 0.028mmole) is dissolved in 35ml of anhydrous pyridine, and phthaloyl chloride (5.81g, 0.034mmole) is added causing immediate precipitation. On mixing and heating under reflux for 1.5h, all dissolves. After cooling, addition of water (42ml) yielded the desired product as a shiny light yellow powder which can used in the next step without further purification. Yield=4.25g(83.1%); mp. 266-268 $^{\circ}$C. ^{1}H-NMR (400 MHz, DMSO-d_6, δ ppm): 8.57 (d, 1H, *J*=2.16Hz, H-4), 8.19 (dd, 1H, *J* = 8.90, 2.4 Hz, H-6), 8.09 (m, 2H, H-1', H-4'), 7.97 (m, 2H, H-2', H-3'), 7.80(d, 1H, *J*=9.40Hz, H-7). ^{13}C-NMR (400 MHz, DMSO-d_6, δ ppm): 168.85, 165.60, 153.66, 123.17, 123.31, 115.20. IR (KBr, cm^{-1}): 3386 (N-H stretching), 3106 (C-H aromatic stretching), 1793, 1728 (N-C=O imide stretching), 1626 (C=N ring stretching), 1423(asymmetric O-N=O stretching), 1344(symmetric O-N=O stretching), 1599, 1474 (skeletal bands). MS (+ESI-QTOF): m/z calculated for $C_{15}H_8N_4O_4$ $[M+H]^+$ 309.24, found 309.2(25.0%).

*4.1.3 General procedure for the synthesis of target compounds (**3a-l**): N-Arylation of free (NH) site in benzimidazole scaffold of intermediate hybridized structure **2**.*

The target compounds were prepared following the literature method. Briefly, mixture of intermediate hybridized structure **2** (1 equiv) and potassium carbonate (2 equiv) in *N*,*N*-dimethylformamide (10mL/mmol) was treated in one portion with the appropriate aryl halide (2 equiv). The reaction mixture was heated under reflux. The reactions usually completed within 2–4 h (monitored by TLC). After the completion of reaction (as evidenced by TLC), reaction mixture cooled to room temperature, and partitioned between ethyl acetate and water. The organic layer was washed with water and brine, dried over sodium sulphate, and concentrated in vacuo. The residue was subjected to silica gel chromatography to give the

desired target compound. The compounds prepared according to this procedure are as follows:

*4.1.3.1 2-(1-(3-Methoxybenzyl)-5-nitro-1H-benzo[d]imidazol-2-yl) isoindoline-1,3-dione (**3a**)*

Compound **3a** was prepared from **2** and 3-methoxybenzyl chloride as a brownish yellow powder. Yield= (0.95g) 65.5%; mp. 242-244°C. ^{1}H-NMR (400 MHz, DMSO-d_6, δ ppm): 7.96 (d, 1H, J=2.16Hz, H-4), 7.82 (dd, 1H, J=8.68, 2.20 Hz, H-6), 7.23-7.19 (m, 2H, H-1', H-4'), 7.09 (s, 2H, H-2', H-3'), 6.82-6.79(m, 3H, H-1'', H-3''and H-4''), 6.73(d, 1H, J=7.68, H-5''), 5.31 (s, 2H, benzylic protons, CH_2). 3.62(s, 3H, $\underline{OCH_3}$). ^{13}C-NMR (400 MHz, DMSO-d_6, δ ppm): 158.66, 157.71, 142.85, 141.92, 139.49, 128.48, 128.38, 128.18, 114.72, 114.03, 109.50, 107.58, 55.03, 44.49. IR (KBr, cm^{-1}): 3108 (C-H aromatics stretching), 2837, 2737(C-H stretching), 1773, 1723 (N-$\underline{C=O}$ imide stretching), 1658(C=N ring stretching), 1431 (asymmetric O-N=O stretching), 1600, 1553, 1462 (skeletal bands), 1398 (symmetric O-N=O stretching), 1254, 1036 (C-O-C stretching). MS (+ESI-QTOF): m/z calculated for $C_{23}H_{16}N_4O_5$ $[M+H]^+$ 429.39, found 429.3(20.0%).

*4.1.3.2 2-(1-(4-Methoxybenzyl)-5-nitro-1H-benzo[d]imidazol-2-yl) isoindoline-1,3-dione (**3b**)*

Compound **3b** was prepared from **2** and 4-methoxybenzyl chloride as a brownish yellow powder. Yield= (0.92) 63.4%; mp. 231-233°C. ^{1}H-NMR (400 MHz, DMSO-d_6, δ ppm): 7.94 (d, 1H, J=2.24Hz, H-4), 7.82 (dd, 1H, J=8.68, 2.20 Hz, H-6), 7.24-7.22 (m, 1H, H-7), 7.19-7.17 (m, 3H, H-1', H-4', H-2'), 7.09(s, 2H, H-1'', H-5''), 6.89-6.85(m, 2H, H-2'', H-4''), 5.30 (s, 2H, benzylic protons, CH_2). 3.70(s, 3H, $\underline{OCH_3}$). ^{13}C-NMR (400 MHz, DMSO-d_6, δ ppm): 159.37, 157.78, 142.84, 142.01, 139.56, 137.83, 129.85, 118.88, 114.80, 113.10, 112.51, 109.86, 107.56, 55.00, 44.91. IR (KBr, cm^{-1}): 3018 (C-H aromatics stretching), 2837, 2738(C-H stretching), 1779 (N-$\underline{C=O}$ imide stretching), 1663(C=N ring stretching), 1430 (asymmetric O-N=O stretching), 1618, 1600, 1480 (skeletal bands), 1329 (symmetric O-N=O

stretching), 1256, 1069 (C-O-C stretching). MS (+ESI-QTOF): m/z calculated for $C_{23}H_{16}N_4O_5$ $[M+H]^+$ 429.397, found 429.3(10.0%).

*4.1.3.3 2-(1-(2-Methylbenzyl)-5-nitro-1H-benzo[d]imidazol-2-yl) isoindoline-1,3-dione (**3c**)*

Compound **3c** was prepared from **2** and 2-methylbenzyl chloride as dark brown powder. Yield= (0.98) 68.2%; mp. 126-128°C. ^{1}H-NMR (400 MHz, DMSO-d_6, δ ppm): 8.00 (d, 1H, J=2.2Hz, H-4), 7.80 (dd, 1H, J=8.7, 2.2 Hz, H-6), 7.25-7.23 (m, 1H, H-7), 7.18-7.12 (m, 1H, H-1'), 7.09-7.10(m, 3H, H-2', H-3', H-2''), 7.04(t, 1H, J=7.2, H-3''), 6.27(d, 1H, J=7.2, H-5''), 5.36 (s, 2H, benzylic protons, CH_2). 2.37(s, 3H, CH_3). ^{13}C-NMR (400 MHz, DMSO-d_6, δ ppm): 158.06, 142.90, 142.03, 139.80, 135.49, 134.02, 132.23, 127.04, 125.95, 123.97, 114.75, 109.57, 107.56, 43.48, 18.63. IR (KBr, cm^{-1}): 3065 (C-H aromatics stretching), 2762 (C-H stretching), 1661 (N-C=O imide stretching), 1477 (asymmetric O-N=O stretching), 1616(C=N ring stretching), 1549, 1408 (skeletal bands), 1321 (symmetric O-N=O stretching). MS (+ESI-QTOF): m/z calculated for $C_{23}H_{16}N_4O_5$ $[MH+Li]^+$ 419.39, found 419.3(80.0%).

*4.1.3.4 2-(1-(3-Methylbenzyl)-5-nitro-1H-benzo[d]imidazol-2-yl) isoindoline-1,3-dione (**3d**)*

Compound **3d** was prepared from **2** and 3-methylbenzyl chloride as brown powder. Yield= (0.98g) 67.5%; mp. 145-147°C. ^{1}H-NMR (400 MHz, DMSO-d_6, δ ppm): 7.96 (d, 1H, *J*=2.24Hz, H-4), 7.84 (dd, 1H, *J*=8.68, 2.24 Hz, H-6), 7.26-7.14 (m, 3H, H-7, H-1', H-4'), 7.15 (s, 2H, H-2', H-3'), 7.09(d, 1H, *J*=7.60, H-3''), 7.03(s, 1H, H-1''), 6.97(d, 1H, *J*=7.68, H-5''), 5.03 (s, 2H, benzylic protons, CH_2). 2.25(s, 3H, CH_3). ^{13}C-NMR (400 MHz, DMSO-d_6, δ ppm): 157.80, 142.84, 141.98, 139.58, 137.83, 136.83, 128.58, 128.26, 127.42, 127.30, 123.94(2C), 114.80, 109.54, 107.53, 44.97, 20.98. IR (KBr, cm^{-1}): 3063 (C-H aromatics stretching), 2837, 2738(C-H stretching), 1776, 1727 (N-C=O imide stretching), 1660(C=N ring stretching), 1450 (asymmetric O-N=O stretching), 1603, 1555, 1479 (skeletal bands),

1321 (symmetric O-N=O stretching). MS (+ESI-QTOF): m/z calculated for $C_{23}H_{16}N_4O_5$ $[M+K]^+$ 451.29, found 451.0.

*4.1.3.5 2-(1-(4-Methylbenzyl)-5-nitro-1H-benzo[d]imidazol-2-yl) isoindoline-1,3-dione (**3e**)*

Compound **3e** was prepared from **2** and 4-methylbenzyl chloride as brownish orange powder. Yield= (1.00g) 68.9%; mp. 135-137°C. ^{1}H-NMR (400 MHz, DMSO-d_6, δ ppm): 7.94 (d, 1H, J=2.24Hz, H-4), 7.83 (dd, 1H, J=8.68, 2.24 Hz, H-6), 7.40 (s, 1H, H-7), 7.26-7.20 (m, 2H, H-1', H-4'), 7.16-7.09(m, 6H, H-2', H-3', H-1'', H-3'', H-4'', H-5''), 5.30 (s, 2H, benzylic protons, CH_2). 2.20(s, 3H, CH_3). ^{13}C-NMR (400 MHz, DMSO-d_6, δ ppm):157.78, 142.83, 141.95, 139.53, 133.24, 129.22, 129.18, 126.95, 126.86, 114.76, 109.51, 107.56, 44.78, 20.60. IR (KBr, cm^{-1}): 3091 (C-H aromatics stretching), 2737(C-H stretching), 1777, 1721 (N-C=O imide stretching), 1661(C=N ring stretching), 1452 (asymmetric O-N=O stretching), 1600, 1553, 1480 (skeletal bands), 1324 (symmetric O-N=O stretching). MS (+ESI-QTOF): m/z calculated for $C_{23}H_{16}N_4O_5$ $[M+H]^+$ 413.39, found 413.0(0.9%).

*4.1.3.6 2-(5-Nitro-1-phenethyl-1H-benzo[d]imidazol-2-yl) isoindoline-1,3-dione (**3f**)*

Compound **3f** was prepared from **2** and 2-phenylethylbenzyl chloride as brown powder. Yield= (0.95g) 65.5%; mp. 258-260°C. ^{1}H-NMR (400 MHz, DMSO-d_6, δ ppm): 8.00 (d, 1H, *J*=2.16 Hz, H-4), 7.77 (dd, 1H, *J*=8.64, 2.20 Hz, H-6), 7.24-7.14 (m, 7H, H-7, H-1', H-2', H-3', H-4', H-2'', H-4''), 7.09-7.07 (m, 1H, H-3''), 6.98(s, 2H, H-1'', H-5''), 4.30 (t, 2H, *J*=7.68Hz, CH_2, H-6'', H-7''). 2.97(t, 2H, *J*=7.64, CH_2, H-8'', H-9''). ^{13}C-NMR (400 MHz, DMSO-d_6, δ ppm): 158.74, 157.37, 149.33, 142.53, 141.70, 139.42, 137.73, 137.63, 133.64, 128.87, 128.12, 128.07, 126.34, 126.29, 117.53, 114.40, 113.18, 109.50, 106.76, 103.49, 43.29, 34.14. IR (KBr, cm^{-1}): 3068 (C-H aromatics stretching), 2743(C-H stretching), 1768 (N-C=O imide stretching), 1665(C=N ring stretching), 1479(C-H methylene bending), 1461 (asymmetric O-N=O stretching), 1598, 1554, 1400(skeletal bands), 1329 (symmetric O-N=O stretching). MS (+ESI-QTOF): m/z calculated for $C_{23}H_{16}N_4O_5$ $[M+K]^+$ 450.39, found 450.2.

*4.1.3.7 2-(5-Nitro-1-(4-vinylbenzyl)-1H-benzo[d]imidazol-2-yl) isoindoline-1,3-dione (**3g**)*

Compound **3g** was prepared from **2** and 4-vinyllbenzyl chloride as brownish orange powder. Yield= (1.03g) 71.0%; mp. 179-181°C. ^{1}H-NMR (400 MHz, DMSO-d_6, δ ppm): 7.97 (d, 1H, J=2.08Hz, H-4), 7.82 (dd, 1H, J=8.68, 2.00Hz, H-6), 7.42-7.35 (m, 3H, H-7, H-1', H-4'), 7.21-7.16 (m, 3H, H-2', H-3', H-2''), 7.10(s, 2H, H-1'', H-5''), 6.67 (dd, 1H, $^{3}J_{trans}$=17.60, $^{3}J_{cis}$=10.92 Hz, vinylic proton, H-1'''), 5.76(d, 1H, J=17.64, vinylic proton, H-2'''), 5.36(s, 2H, benzylic protons, CH_2), 5.23(d, 1H, J=10.96, vinylic proton, H-3'''). ^{13}C-NMR (400 MHz, DMSO-d_6, δ ppm): 157.73, 142.85, 142.06, 139.44, 136.43, 135.97, 135.73, 127.10, 127.02, 126.51, 126.25, 114.67, 114.21, 113.49, 107.27, 103.75, 103.75, 44.88. IR (KBr, cm^{-1}): 3086 (C-H aromatics stretching), 2743(C-H stretching), 1777 (N-C=O imide stretching), 1660(C=N ring stretching), 1629 (C=C vinylnic stretching), 1454 (asymmetric O-N=O stretching), 1600, 1553, 1479(skeletal bands), 1325 (symmetric O-N=O stretching), 994, 918 (C-H out of plane bending). MS (+ESI-QTOF): m/z calculated for $C_{24}H_{16}N_4O_4$ $[M+H]^+$ 425.40, found 425.0(4.2%).

*4.1.3.8 2-(1-(4-Isopropylbenzyl)-5-nitro-1H-benzo[d]imidazol-2-yl)isoindoline-1,3-dione (**3h**)*

Compound **3h** was prepared from **2** and 4-isopropylbenzyl chloride as yellow powder. Yield= (1.00g) 68.9%; mp. 265-267°C. ^{1}H-NMR (400 MHz, DMSO-d_6, δ ppm): 8.00 (d, 1H, *J*=2.2 Hz, H-4), 7.82 (dd, 1H, *J*=8.6, 2.2 Hz, H-6), 7.20-7.10 (m, 7H, H-7, H-1', H-4', H-2', H-3', H-2'', H-4''), 6.96 (s, 2H, H-1'', H-5''), 5.30 (s, 2H, benzylic protons, CH_2), 2.80 (sep, 1H, *J*=6.90 Hz, isopropyl methine proton), 1.20(d, 6H, *J*=6.88Hz, isopropyl methyl protons). ^{13}C-NMR (400 MHz, DMSO-d_6, δ ppm): 157.62, 147.74, 142.72, 142.08, 139.34, 133.16, 126.59, 126.51, 126.34, 114.65, 109.83, 106.94, 44.98, 33.12, 23.64. IR (KBr, cm^{-1}): 3090 (C-H aromatics stretching), 2965, 2870(C-H stretching), 1765 (N-C=O imide stretching), 1660 (C=N ring stretching), 1431 (asymmetric O-N=O stretching), 1322, 1301 (C-H gem-

dimethyl bending), 1617, 1550 (skeletal bands). MS (+ESI-QTOF): m/z calculated for $C_{25}H_{20}N_4O_4$ $[M+H]^+$ 441.44, found 441.0(3.3%).

*4.1.3.9 2-(1-(4-(tert-Butyl) benzyl)-5-nitro-1H-benzo[d]imidazol-2-yl) isoindoline-1,3-dione (**3i**)*

Compound ***3i*** was prepared from **2** and 4-*tert*-butyl benzyl chloride as dark yellow powder. Yield= (1.01g) 70.0%; mp. 189-191°C. ^{1}H-NMR (400 MHz, DMSO-d_6, δ ppm): 7.95 (d, 1H, J=2.20 Hz, H-4), 7.82 (dd, 1H, J=8.68, 2.2 Hz, H-6), 7.33-7.31 (m, 3H, H-1', H-4', H-2''), 7.23(d, 1H, J=8.68, H-7), 7.11-7.13 (m, 2H, H-2', H-3'), 7.05 (s, 2H, H-1'', H-5''), 5.30 (s, 2H, benzylic protons, CH_2), 1.20(s, 9H, *tert*-butyl). ^{13}C-NMR (400 MHz, DMSO-d_6, δ ppm): 157.74, 149.91, 142.85, 142.02, 140.56, 139.51, 133.16, 126.52, 126.44, 125.26, 114.65, 109.61, 107.29, 44.73, 34.11, 31.00. IR (KBr, cm^{-1}): 3092 (C-H aromatics stretching), 2959, 2743(C-H stretching), 1773 (N-C=O imide stretching), 1661(C=N ring stretching), 1431 (asymmetric O-N=O stretching), 1383, 1336 (C-H *tert*-butyl bending), 1601, 1553, 1458 (skeletal bands). MS (+ESI-QTOF): m/z calculated for $C_{26}H_{22}N_4O_4$ $[M+H]^+$ 455.45, found 455.0(4.2%).

*4.1.3.10 2-(1-([1,1'-Biphenyl]-3-ylmethyl)-5-nitro-1H-benzo[d]imidazol-2-yl)isoindoline-1,3-dione (**3j**)*

Compound ***3j*** was prepared from **2** and 3-phenylbenzyl chloride as yellow brownish powder. Yield= (1.02g) 70.3%; mp. 247-249°C. ^{1}H-NMR (400 MHz, DMSO-d_6, δ ppm): 7.98 (d, 1H, *J*=2.2 Hz, H-4), 7.84 (dd, 1H, *J*=8.68, 2.2 Hz, H-6), 7.57-7.52 (m, 5H, H-7, H-1', H-4', H-2', H-3'), 7.45-7.39 (m, 4H, H-1'', H-3'', H-4'', H-5''), 7.37-7.34 (m, 2H, H-1''', H-5'''), 7.30-7.27 (m, 1H, H-3'''), 7.15-7.13(m, 2H, H-2''', H-4'''), 5.50 (s, 2H, benzylic protons, CH_2). ^{13}C-NMR (400 MHz, DMSO-d_6, δ ppm):157.66, 142.85, 142.12, 140.63, 139.81, 139.46, 136.84, 129.13, 128.75, 127.42, 126.55, 125.86, 125.71, 125.62, 125.49, 114.72, 109.14, 107.27, 45.17. IR (KBr, cm^{-1}): 3063 (C-H aromatics stretching), 2739(C-H stretching), 1778

(N-C=O imide stretching), 1661(C=N stretching), 1445 (asymmetric O-N=O stretching), 1599, 1511, 1455 (skeletal bands), 1322 (symmetric O-N=O stretching). MS (+ESI-QTOF): m/z calcd for $C_{28}H_{18}N_4O_4$ $(M+H)^+$ 475.46, found 475.1(3.3%).

*4.1.3.11 2-(5-Nitro-1-(4-nitrobenzyl)-1H-benzo[d]imidazol-2-yl) isoindoline-1,3-dione (**3k**)*

Compound ***3k*** was prepared from **2** and 4-nitrobenzyl chloride as brownish orange powder. Yield= (0.84g) 57.9%; mp. 188-190°C. ^{1}H-NMR (400 MHz, DMSO-d_6, δ ppm): 8.20-8.15 (m, 3H, H-2'', H-4'', H-7), 8.00(1H, d, *J*=2.16, H-4), 7.82 (dd, 1H, *J*=8.64, 2.20 Hz, H-6), 7.42-7.40 (m, 3H, H-1', H-4', H-2'), 7.21-7.18(m, 1H, H-3'), 7.11 (s, 2H, H-1'', H-5''), 5.53 (s, 2H, benzylic protons, CH_2). ^{13}C-NMR (400 MHz, DMSO-d_6, δ ppm): 157.57, 146.85, 143.75, 142.88, 142.30, 139.20, 127.79, 123.57, 114.75, 109.88, 107.04, 44.61. IR (KBr, cm^{-1}): 3063 (C-H aromatics stretching), 2754(C-H stretching), 1664 (N-C=O imide stretching), 1475 (asymmetric O-N=O stretching), 1618 (C=N stretching) 1554, 1503 (skeletal bands), 1324 (symmetric O-N=O stretching). MS (+ESI-QTOF): m/z calculated for $C_{22}H_{13}N_5O_6$ $[M+H]^+$ 444.36, found 444.1(2.5%).

*4.1.3.12 2-(5-Nitro-1-(2-nitrobenzyl)-1H-benzo[d]imidazol-2-yl) isoindoline-1,3-dione (**3l**)*

Compound ***3l*** was prepared from **2** and 2-nitrobenzyl chloride as a yellowish brown powder. Yield= (0.91g) 62.7%; mp. 210-212°C. ^{1}H-NMR (400 MHz, DMSO-d_6, δ ppm): 8.18-7.92(m, 2H, H-4, H-2''), 7.84 (dd, 1H, *J*=8.64, 2.26Hz, H-6), 7.50-7.52(m, 1H, H-7), 7.37-7.31 (m, 3H, H-1', H-4', H-3''), 7.21-7.16(m, 3H, H-2', H-3', H-4''), 7.10(s, 1H, H-5''), 5.53 (s, 2H, benzylic protons, CH_2). ^{13}C-NMR (400 MHz, DMSO-d_6, δ ppm): 158.46, 149.47, 139.25, 138.73, 133.59, 130.38, 130.24, 129.53, 125.58, 125.41, 121.95, 118.82, 113.57, 103.64, 44.24. IR (KBr, cm^{-1}): 3070 (C-H aromatics stretching), 2754 (C-H stretching), 1664 (N-C=O imide stretching), 1475 (asymmetric O-N=O stretching), 1618 (C=N stretching), 1554 (skeletal bands), 1324 (symmetric O-N=O stretching). MS (+ESI-QTOF): m/z calculated for $C_{22}H_{13}N_5O_6$ $(M+K)^+$ 481.37, found 481.4.

4.2. Biological evaluation (Experiments in vitro)

4.2.1 Material and method

COX (ovine/human) inhibitor screening assay kit procured commercially from Cayman suppliers. All materials, chemicals, drugs and reagents used in this experiments were purchased from Sigma-Aldrich Co, (St Louis, MO, USA). For *In vitro* TNF-α inhibition activity, Mouse TNF-alpha ELISA kit (Cat No: ELM-TNFα-1, Make: RayBiotech, USA) procured commercially from suppliers. RAW (Mouse macrophages) cell line were procured from National Centre for Cell Sciences (NCCS), Pune, India. Fetal Bovine Serum (FBS), penicillin, MEM/DMEM, streptomycin, amphotericin B procured from Gibco, Hi-Media. For lipoxygenase inhibitory activity, Human recombinant 5-LOX (Item no: 60402) procured from Cayman suppliers, Lipoxidase (LOX) type 1-B from Glycine max (soybean) purchased from Sigma-Aldrich Co, (St Louis, MO, USA). Boric acid, linoleic acid, NaOH, ethanol, NDGA, Tris buffer, $CaCl_2$, 0.1mM EDTA, ATP and DMSO were obtained from Sigma-Aldrich Co, (St Louis, MO, USA).

4.2.2. In vitro COX-1 and COX-2 inhibitory assay

All the newly synthesized compounds were screened for their ability to inhibit COX-1 and COX-2 enzymes. This was carried out using Cayman colorimetric COX (ovine) inhibitor screening assay kit (Catalog No. 760111) supplied by Cayman chemicals, Ann Arbor, MI, USA, according to reported method [16].

4.2.3. In vitro human recombinant 5-lipoxygenase (LOX) assay

All the newly synthesized compounds were screened for their ability to inhibit human recombinant 5-LOX enzyme. Recombinant LOX activity assays were performed at room temperature as reported previously. The newly generated conjugated diene (HETEs and HpETEs) catalyzed by LOXs can be detected by the absorbance at 234 nm using an ultraviolet visible spectrophotometer Hitachi U2900 (Tokyo, Japan) (assay buffer: 50mM

Tris-Buffer (pH=7.5) containing 2mM EDTA, 2mM $CaCl_2$, 2mM ATP). All enzyme reactions were carried out in 1 cm path length quartz cuvettes with a total volume of 2 mL, and absorbance at 234 nm was continuously measured for 300s. To determine the inhibitor activity, various concentrations of test compounds were used, and the reaction was started by the introduction of 20mM linoleic acid [17].

4.2.4. *In vitro 15-lipoxygenase assay procedure*

The ability of the test compounds to inhibit human 15-LOX (IC_{50} value, µM) listed in Table 1. Lipoxidase (LOX) type 1-B from Glycine max (soybean), boric acid, linoleic acid, NaOH, ethanol (96%) were used with no further purification. LOX inhibition activity was determined spectrophotometrically by measuring the increase in absorbance at 234 nm for the oxidation of linoleic acid. The reaction mixture contained (final concentration) the test compounds, dissolved in DMSO at concentrations of 0.01–100 µM, or the solvent (control) and linoleic acid 152 µM, in borate buffer (pH = 9.0). The reaction was started by adding a lipoxygenase in amount of 500 units. Five different concentrations of each test compounds were used for the inhibition activity experiments. The increase in absorbance was recorded for 300 s under controlled temperature 25ºC [18].

4.2.5. *In vitro TNF-alpha assay procedure*

The ability of the test compounds to inhibit TNF-alpha (IC_{50} value, µM) listed in Table 1. RAW cells seeded in to 6 well culture dishes at a cell population of 1.5 to $2x10^5$ cells/ml in DMEM with 10% FBS. After 24 h, the cells were treated with range of test concentrations of test compounds along with 1µg/ml of lipopolysaccharide (LPS) and incubated at 37ºC with 5% $CO_2$for 4 h. After incubation, the cell supernatant was collected, centrifuged, separated and stored at -20º C till use. The TNF-alpha levels in the cell supernatants were estimated by using standard ELISA kit specific for mouse (Mouse TNF-alpha ELISA, Cat No: ELM-TNFα-1, Make: Ray Biotech, USA) as per the standard kit protocol. Based on the estimated

quantities of TNF-alpha against control group, percentage inhibition of TNF-alpha were determined against control [19].

4.2.6 In vivo assay

4.2.6.1. Animals

Albino Wistar rats of either sex (150-330g) were obtained from Central Animal House, Punjabi University, Patiala. All animals accessed food and water *ad libitum* and were housed in 12h dark/light cycle in a controlled at room 23-25°C. They were allowed to acclimatize to the experiment room 2hr before the experiment. Experiments were carried out using protocols approved by Institutional Animal Ethics Committee (registration number 107/GO/ReBi/99/CPSCEA) and care of animals carried out as per the Committee for the Purpose of Control And Supervision of Experiments on Animals (CPSCEA). On the same set of animals *in vivo* tests proposed to be carried out. In all tests, adequate considerations were used to reduce discomfort or pain of animals.

4.2.6.2. Drugs

Indomethacin, Celecoxib, Carrageenan, Craboxymethylcellulose were purchased from Sigma-Aldrich Chemicals Pvt. Limited, Bangalore, India. The novel compounds were synthesized based on the previously described methods.

4.2.6.3. Preparation of samples for bioassay

Unless otherwise stated, the conditions are employed in all experiments. Test samples will be given orally to test animals after suspending in 0.5% sodium carboxymethylcellulose. The control group animals receives the same experimental handling as those of the test groups except that the drug treatment is replaced with appropriate volumes of the dosing vehicle. Both indomethacin and celecoxib in 0.5% sodium carboxymethyl cellulose were served as standard drugs. The test compound (**3j**) administered on molar equivalent basis of reference standards.

4.2.6.4. *Anti-inflammatory assay*

Compound **3j** was evaluated for its *in vivo* anti-inflammatory activity applying the carrageenan-induced paw edema model reported previously [20]. Rats were randomly divided to five groups (*n*=6). The rats in group I (normal control) was kept as non-immunized untreated. Rats that were given the vehicle (0.5% sodium carboxymethylcellulose) served as carrageenan control group (group II).The other groups (group III, IV and V) were orally administered the drugs—indomethacin and celecoxib as reference standards at a dose 0.05mmol/kg of body weight and the tested compound **3j** (equimolar dosage to reference standards). After 45 minutes, in all groups apart from the normal control, the rat paw oedema induced by injected 100µl of carrageenan solution subcutaneously into sub plantar tissue of the right hind paw. The paw volume were measured using plethysmometer in different treatment groups, 3hr and 5hr following the carrageenan injection. The increase in paw volume was calculated by subtracting the volumes before and 3hr and 5hr after the injection of carrageenan. Edema was expressed as an increase in the volume of paw, and the percentage of edema inhibition (or percent protection against inflammation) for each rat and each rat was calculated according to the following equation:

% Inhibition= $(V_t\text{-}V_0)$ control-$(V_t\text{-}V_0)$ test compound/ $(V_t\text{-}V_0)$ control X 100

Where V_t is the mean volume of edema at specific time interval (after 3hr and 5hr) and V_0 is the mean volume of edema at zero time interval.

4.2.6.5. *Analgesic assay*

Compound **3j** was evaluated for its in vivo analgesic activity using 4% sodium chloride writhing (abdominal constriction) assay as described previously [21]. The analgesic activity of the compounds was done at the same dose as used for anti-inflammatory activity. In this model, at the time interval of 3hr after the oral administration of dosing vehicle (control), reference standards (indomethacin and celecoxib) or test sample (**3j**) the writhing responses

were induced by intraperitoneal injection of 4% sodium chloride solution to groups of six rats each. For each animal the total number of abdominal constrictions (writhes) will be counted for the next 10 min, starting on the fifth minute after the 4% sodium chloride injection and is expressed as writhing numbers. Percent inhibition of writhing was also calculated and compared among control and drug-treated groups.

4.2.6.6. *Gastric ulcerogenic activity*

Compound **3j** was further evaluated for acute gastric ulcerogenic risk evaluation using indomethacin-induced gastric ulcer model [22]. This was done at three times higher dose in comparison to the dose used for anti-inflammatory activity, i.e. 0.15mmol/kg of body weight of indomethacin and the test compound were used. Each group had three animals which were later scarificed according to CPSCEA guidelines. Their stomach is removed, opened along the greater curvature, washed with saline, carefully examined and ulcers were scored according to severity as follows:

Normal colored stomach-0, Red coloration-0.5, Spot ulcers-1.0, Hemorrhagic streaks-1.5, Ulcers >3mm but <5mm-2.0, Ulcers>5mm-3.0

4.2.6.7. *Lipid peroxidation assay*

Lipid peroxidation studies were carried out according to the previously reported method [23]. After scoring the gastric mucosa of animals for ulcerogenic effect of synthesized drugs, the gastric mucosa of animals was scraped with two glass slides, weighed (100 mg), and homogenized in 1.8 mL of 1.15% ice-cold potassium chloride (KCl) solution. The homogenate was supplemented with 0.2 mL of 8.1% sodium dodecyl sulphate (SDS), 1.5 mL of acetate buffer (pH 3.5), and 1.5 mL of 0.8% thiobarbituric acid (TBA). The mixture was heated at 95°C for 60 min. The cooled reactants were shaken vigorously for 1 min and centrifuged for 10 min at 4000 rpm after supplementing with 5 mL of a mixture of *n*-butanol and pyridine (15:1 v/v). The supernatant organic layer was collected and absorbance was

measured at 532 nm on UV spectrophotometer. The results are expressed as nmoles of malondialdehyde (MDA)/100 mg tissue, using extinction coefficient 1.56×10^5 per cm/M.

4.3 Anti-inflammatory docking study

Molecular docking analysis was performed using CDOCKER algorithm to find the binding mode for synthesized molecules with target proteins. CDOCKER has been incorporated into Discovery Studio 4.1 (Accelrys Software Inc., San Diego, CA) through the Dock Ligands (CDOCKER) protocol. We extracted the crystal structure of COX-2, COX-1, 15-LOX and 5-LOX (PDB ID: 6COX, 1PGF, 1IK3 and 3V99, respectively) from the RCSB Protein Data Bank [http://www.rcsb.org/pdb]. In CDOCKER, random ligand conformations were generated from the initial ligand structure through high-temperature molecular dynamics followed by random rotations. Then, the random conformations were refined by grid-based simulated annealing, which makes the results more accurate. The CDOCKER interaction energy was then computed between the ligands and target proteins. The docking analysis provided insights into the interactions between the synthesized molecules and target proteins, which facilitated in mechanistic justification of the obtained biological results.

4.4. *Statistical Analysis*

Statistical analyses were performed with GraphPad Prism 5.0 (GraphPad Software, Inc., San Diego, CA). Data are expressed as mean and standard deviation± SD. Parametric test, one-way analysis of variance (ANOVA) and the Tukey post hoc test were performed on the data for intergroup comparisons besides two-way analysis of variance (ANOVA) followed by Bonferroni post hoc test. Nonparametric tests, Kruskal-Wallis test and Mann–Whitney test were used to compare ulcerogenicity in different groups. The nominal statistical significance level was set at 0.05.

Conflict of interest

There are no conflicts to declare.

Acknowledgements

The author(s) thank research group of Molecular Modelling Lab, Department of Pharmaceutical and Drug Research, Punjabi University Patiala, for the helpful discussion and suggestions during the redaction of this paper.

Notes and References

[1] P.P.N Rao and E.E Knaus. J.Phar Pharmaceut Sci. 11**(**2008) 81s- 110s.

[2] (a) G. Mathew, M. K. Unnikrishnan, Inflamm. Res. 64**(**2015) 747–752. (b) R. Morphy and Z. Rankovic, J. Med. Chem. 48**(**2005) 6523-6543. (c) G. Kaur, O. Silakari, Future Med Chem. 9**(**2017) 1361-1376.

[3] P. L. Bosquesi, T. R. F. Melo, E. O. Vizioli, J. L. Dos Santos, M. C. Chung, Pharmaceuticals. 4**(**2011)1450–1474.

[4] D.A Horton, G.T Bourne, M.L Smythe, Chem. Rev. 103**(**2003) 893-930.

[5] G. Kaur, M. Kaur, O. Silakari, Mini. Rev. Med. Chem, 14**(**2014)747–767.

[6] T. Ito, H. Ando, T. Suzuki, T. Ogura, K. Hotta, Y. Imamura, Y. Yamaguchi, H. Handa, Science, 327**(**2010)1345-1350.

[7] T.M Ehrman, D.J Barlow, P.J Hylands, Bioorg. Med Chem. 18**(**2010) 2204- 2218.

[8] F. Lovering and Y. Zhang, Curr. Drug Targets CNS Neurol. Disord. 4**(**2005)161–168.

[9] K. Brune, Rheumatology. 43S (2004)i16–i20.

[10] (a) P.S Penglis, L.G Cleland, M Demasi, G.E Caughey, M.G James, J Immunol, 165**(**2000)1605–1611. (b) S. Sacco, D. Agnello, M. Sottocorno, G. Lozza, A. Monopoli, P. Villa, P. Ghezzi, J Neurochem. 71**(**1998)2063-70. (c) T.H Page, J.J Turner, A.C Brown, E.M Timms, J.J Inglis, F.M Brennan, B.M Foxwell, K.P Ray , M. Feldmann, J Immunol. 185**(**2010)3694-701.

[11] J. Martel-Pelletier, D. Lajeunesse, P. Reboul, J.P Pelletier, Ann Rheum Dis. 62 (2003)501-99.

[12] C. Ezerzer, M. Dolgin, J. Skovorodnikova, N. Harris, Peptides. 30**(**2009)1296-1305.

[13] (a) M. Bella, V. Milata, L.I. Larina, J. Heterocycl. Chem. 49**(**2012)293–296. (b) Y.F Li, G.F Wang, Y. Luo, W.G Huang, W. Tang, C.L Feng, L.P Shi, Y.D Ren, J.P Zuo, W. Lu, Eur. J. Med. Chem. 42**(**2007)1358-1364.

[14] (a) A. R Katritzky, F. Yates, J. Chem. Soc. Perkin Trans. 1(1976)309.

[15] (a) M.M Ramla, M.A Omar, H. Tokuda, H.I El-Diwani, Bioorg Med Chem. 15**(**2007) 6489-6496. (b) A.R Porcari, R.V Devivar, L.S Kucera, J.C Drach, L.B Townsend, J Med Chem. 41**(**1998) 1252-62. (c) J.P Powers, S. Li, J.C Jaen, J.Liu , N.P Walker, Z. Wang, H. Wesche, Bioorg Med Chem Lett. 16**(**2006) 2842-5.

[16] (a) W.L Xie, J.G Chipman, D.L Robertson, R.L Erikson, and D.L Simmons, Proc. Natl. Acad. Sci, 88**(**1991)2692-2696. (b) A.L Blobaum and L.J Marnett, J. Med. Chem. 50**(**2007) 1425-1441.

[17] (a) R. Wisastra, M. Ghizzoni, A. Boltjes, H.J. Haisma, F.J. Dekker, Bioorg Med Chem. 21(2013)7763-78. (b) E.K. Hoobler, G. Rai , A.G. Warrilow, S.C. Perry, C.J. Smyrniotis, A. Jadhav, A. Simeonov, J.E. Parker, D.E. Kelly, D.J. Maloney, PloS one. 8**(**2013) e65928. (c) I.A. Butovich, S.M. Lukyanova, J Lipid Res. 49 (2008) 1284–94. (d) J.H. Suh, E.K. Yum, Y.S. Cho. Chem Pharm Bull. 63**(**2015) 573-8.

[18] (a) K. Surrey, Plant Physiol. 39**(**1964) 65–70. (b) A.T. Evans, E.A. Formukong, F.J. Evans, Biochem Pharmacol. 36**(**1987) 2035–7. (c) R. Wisastra, M. Ghizzoni, A. Boltjes, H.J. Haisma, F.J. Dekker, Bioorg Med Chem. 20**(**2012) 5027-32.

[19] (a) D. Francis and L. Rita, J Immunol Methods. 89(1986) 271-277. (b) R.S. Varma, G. Ashok, S. Vidyashankar, P. Patki, K.S. Nandakumar, Immunopharmacol Immunotoxicol, 33**(**2011)55-63.

[20] (a) C.A. Winter, E.A. Risley, G.W. Nuss, Proc Soc Exp Biol Med. 111**(**1962)544- 7. (b) H.H. Cong, V.N. Khaziakhmetova, L.E. Zigashina, Int J Risk Saf Med. 27**(**2015) S76-7. (c) S. Haider, M.S. Alam , H. Hamid, S. Shafi , A. Nargotra , P. Mahajan, S. Nazreen , A.M. Kalle , C. Kharbanda , Y. Ali , A. Alam , A.K. Panda, Eur. J. Med. Chem. 70(2013)579-588.

[21] (a) K. Fukawa , O. Kawano , M. Hibi , N. Misaki , S. Ohba , Y. Hatanaka, J Pharmacol Methods. 4**(**1980) 251–259. (b) A.G. Habeeb, P.N. Praveen Rao, E.E. Knaus, J. Med. Chem. 44(2001)2921–2927.

[22] (a) V. Cioli, S. Putzolu , V. Rossi , S.P. Barcellona, C. Corradino, Toxicol Appl Pharmacol. 50**(**1979)283-289. (b) T. Corell, J.K. Moller, J. Splawinski, Acta pharmacol. Toxicol. 45**(**1979) 232–239.

[23](a) H. Ohkawa, N. Ohishi, K. Yagi, Anal Biochem, 95(1979)351–358. (b) J. Tanaka, Y. Yuda, Biol Pharm Bull. 19**(**1996)716–20.

Figure captions

Figure 1. Design strategy of benzimidazole scaffold based hybrid molecules. Identified pharmacophoric elements for COX inhibitors (IA), LOX inhibitors (IIB) and TNF-α inhibitors (IIIC) highlighted in rectangular framework (blue color). Proposed benzimidazole scaffold based hybridized structure (IV) that, under one construct, combines identified pharmacophoric elements that characterize well known classes of COX, LOX and TNF-α inhibitors via rational molecular hybridization drug design strategy. Further in order to investigate the effect of molecular variation at the D framework of the designed hybridized

structure on the *in vivo*/*in vitro* anti-inflammatory activity, series of 12 compounds generated for SAR studies.

Figure 2. (A) Typical representative macroscopic photographs of paw from the (**a**) Normal control (noninflammed, untreated), (**b**) 1.0% carrageenan + vehicle (carrageenan control), (**c**) 1.0% carrageenan + celecoxib and (**d**) 1.0% carrageenan + Test compound (3j) groups. (B) Treated groups versus paw edema (mL) at after 3 h and after 5 h. Values were expressed as mean ± SD six rats/group. Data was analysed by Two way ANOVA followed by post hoc test. (**P* < 0.001 vs. Normal Control; [a]*P* < 0.001 vs. Carrageenan Control; [b]*P* < 0.01 vs. Celecoxib; [#] No statistical difference was found vs. 3j)

Figure 3. Docked pose of interactions of compound **3j** with COX-2 active site (6COX) using CDOCKER algorithm.

Figure 4. Docked pose of interactions of compound **3j** with 5-LOX active site (3V99) using CDOCKER algorithm.

Figure 5. Docked pose of interactions of compound **3j** with 15-LOX active site (1IK3) using CDOCKER algorithm.

Figure 6. Docked pose of interactions of compound **3c** with COX-1 active site (1PGF) using CDOCKER algorithm.

Scheme 1(A). Synthetic pathway to target compounds (**3a-l**). Reagents and conditions: (i) BrCN, H_2O, Reflux; (ii) *o*-phthaloyl dichloride, dry pyridine, reflux; (iii) Aryl halide, K_2CO_3, DMF, Reflux. **(B).** Plausible reaction mechanism.

Table 1. *In vitro* cyclooxygenases, lipoxygenases and TNF-α inhibition data for compounds (**3a-l**).

Table 2. Anti-inflammatory data of the 2-(1-([1,1'-Biphenyl]-3-ylmethyl)-5-nitro-1*H*-benzo[d]imidazol-2-yl)isoindoline-1,3-dione (**3j**) on carrageenan-induced paw edema in rat.

Table 3. Analgesic, ulcerogenic and lipid peroxidation activities of the compound **3j.**

Table S1. Physicochemical and TLC data of synthesized target compounds.

Table S2. *In vivo* anti-inflammatory activity of **3j** in carrageenan-induced paw edema model.

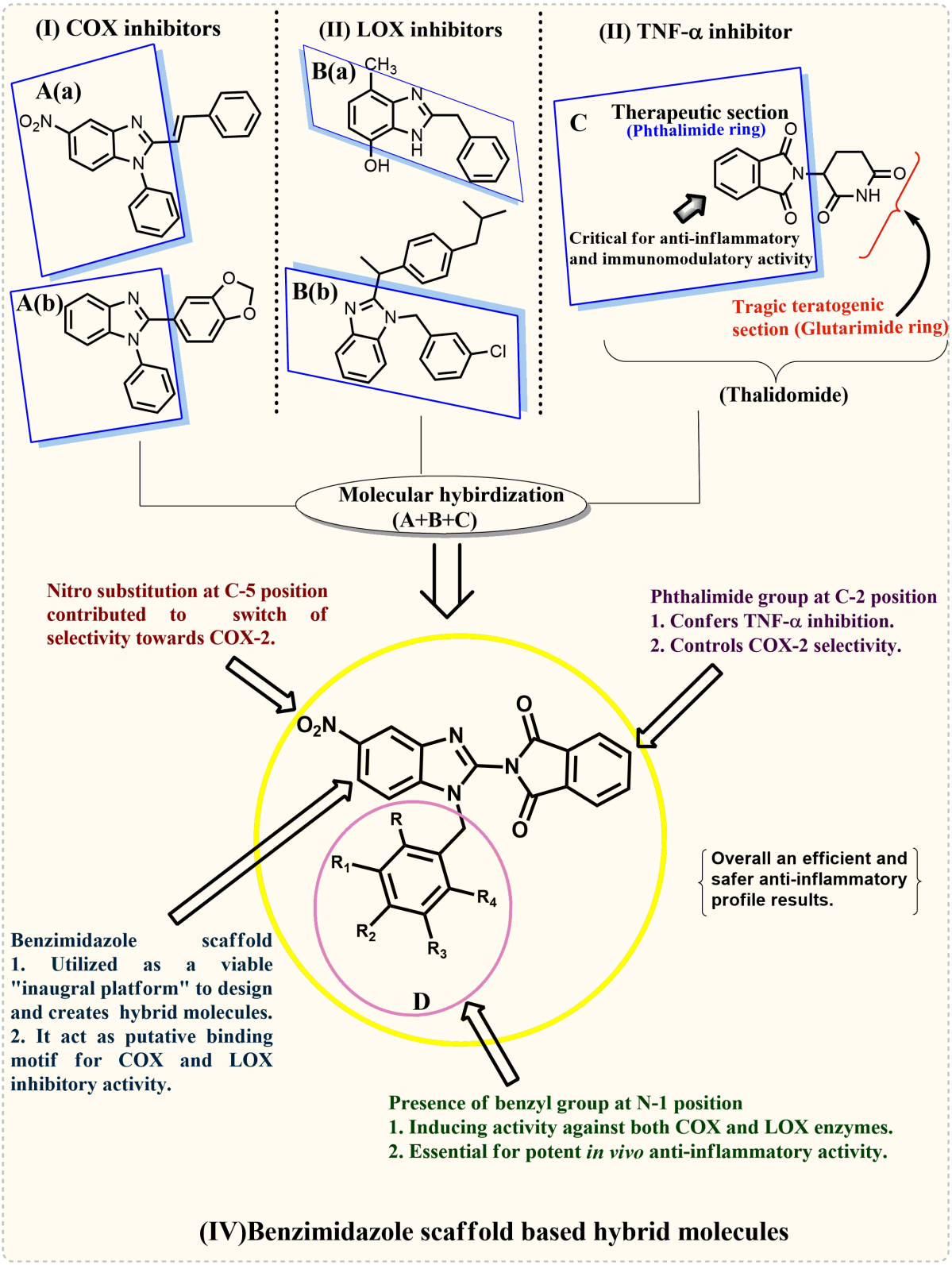

(IV)Benzimidazole scaffold based hybrid molecules

(A)

(a) Normal control group

(b) Carrageenan control group

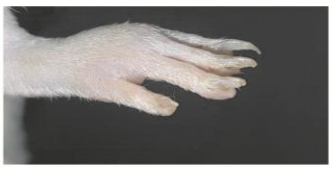

(c) Reference standard (celecoxib)

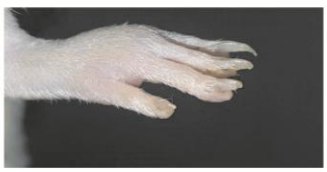

(d) Test compound (3j)

(B)

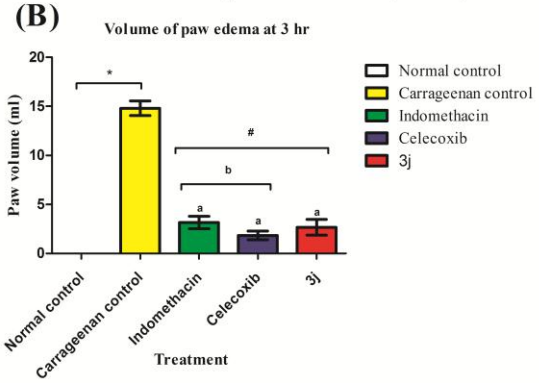

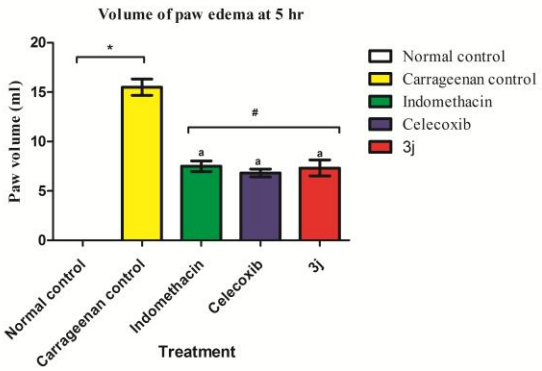

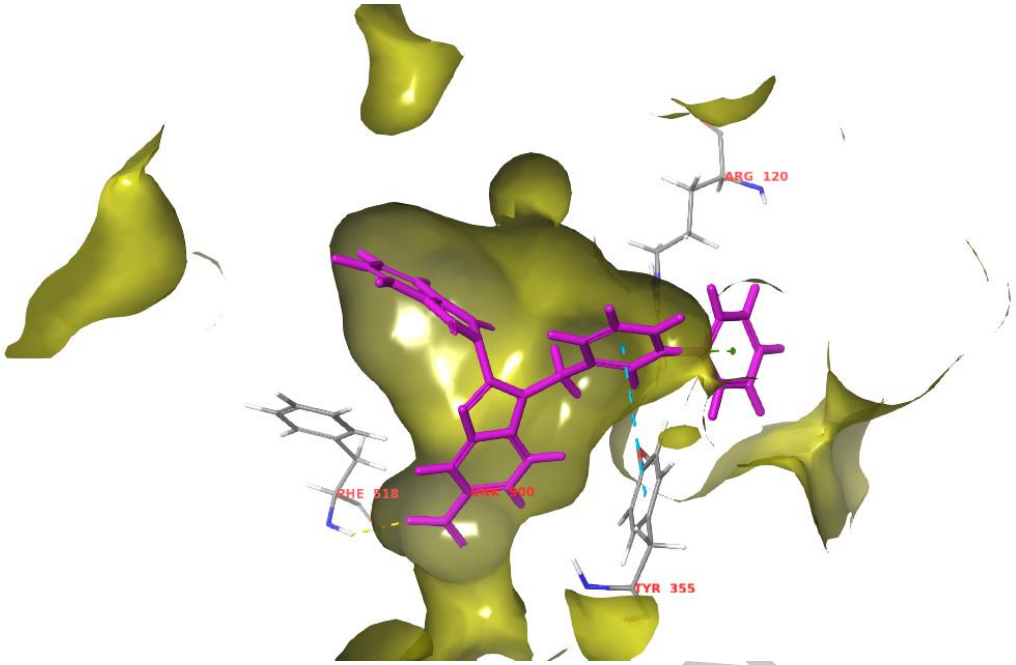

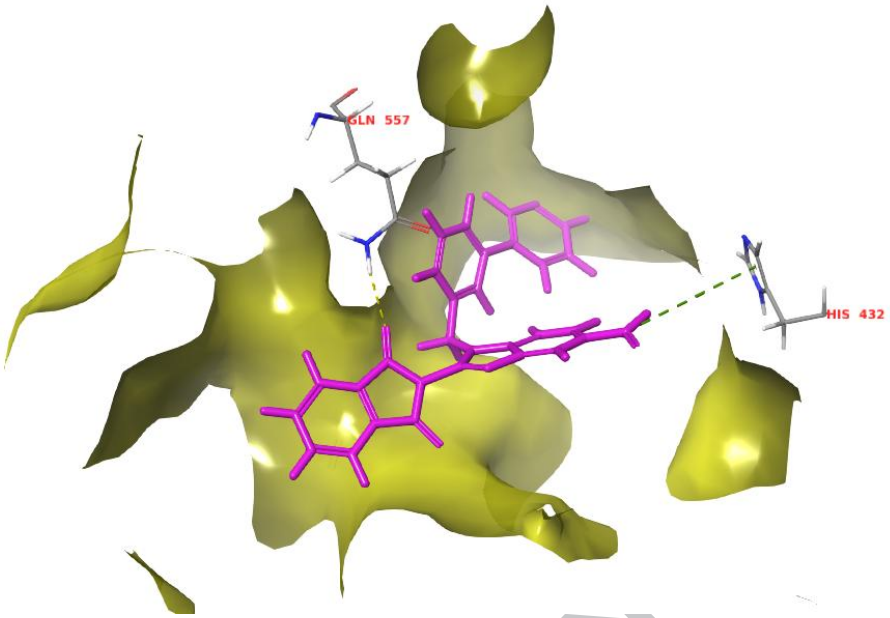

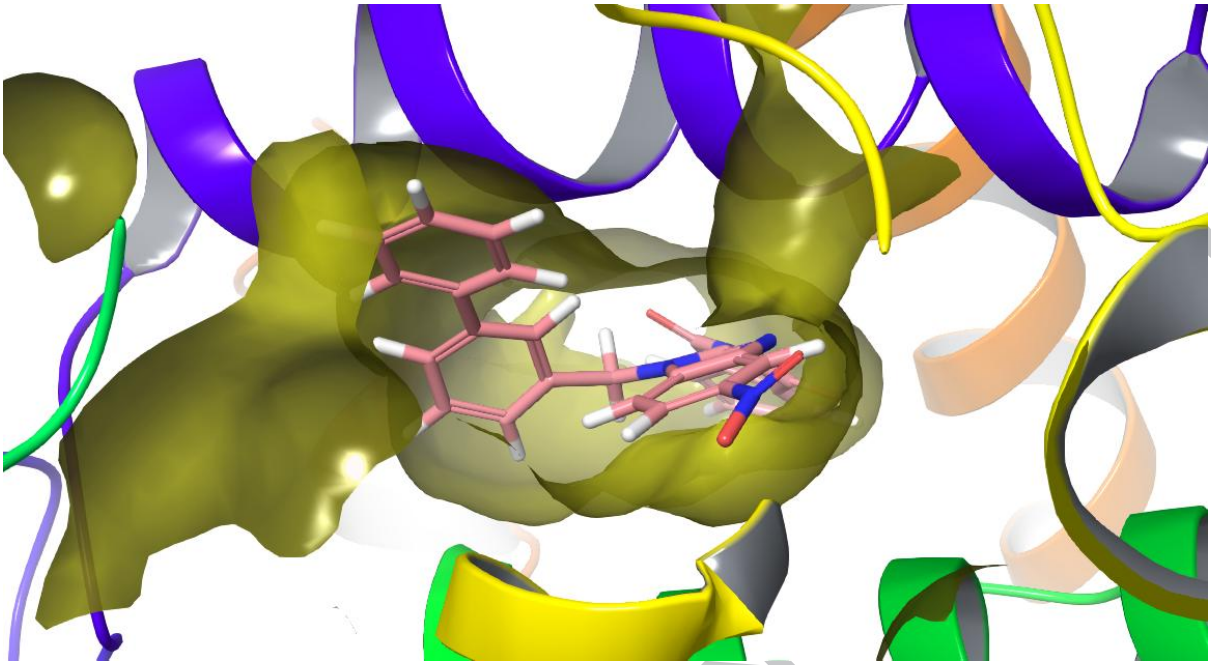

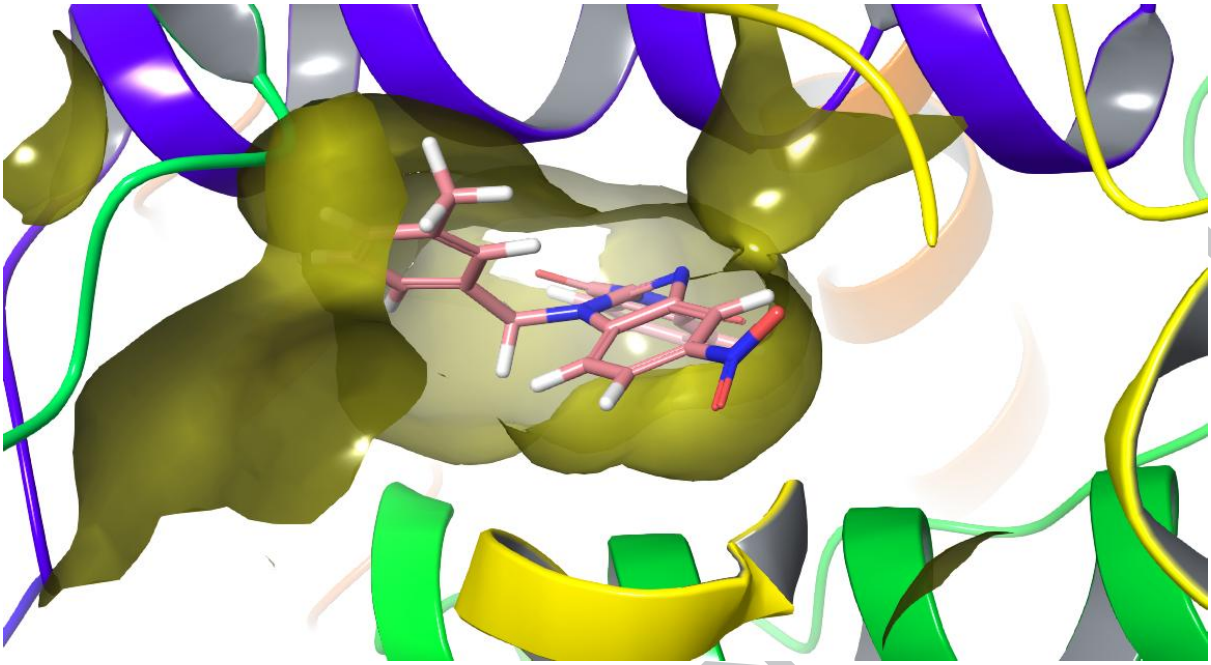

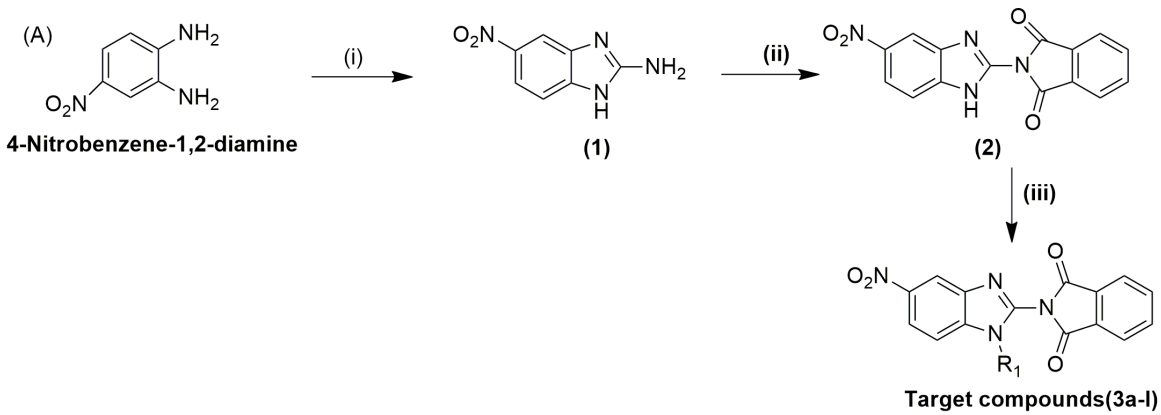

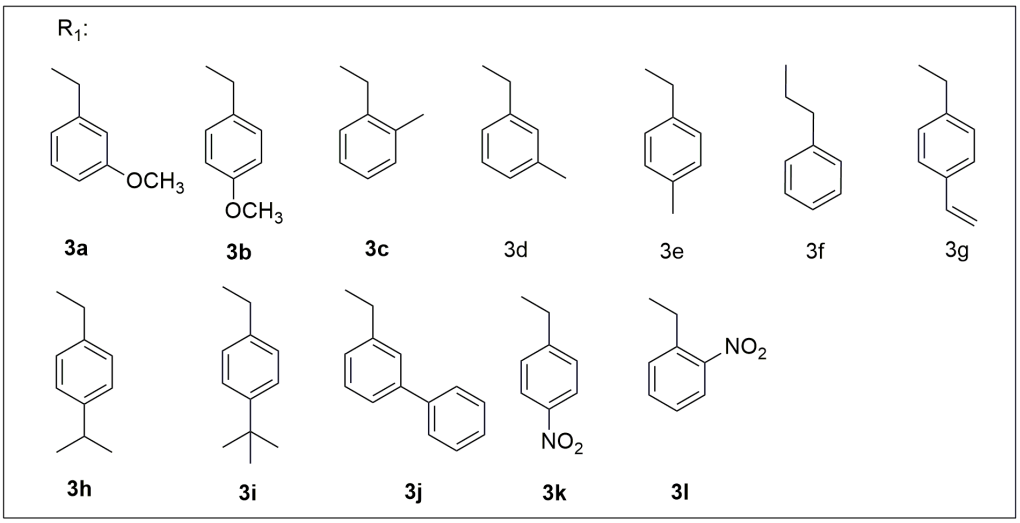

(B) **Plausible reaction mechanism**

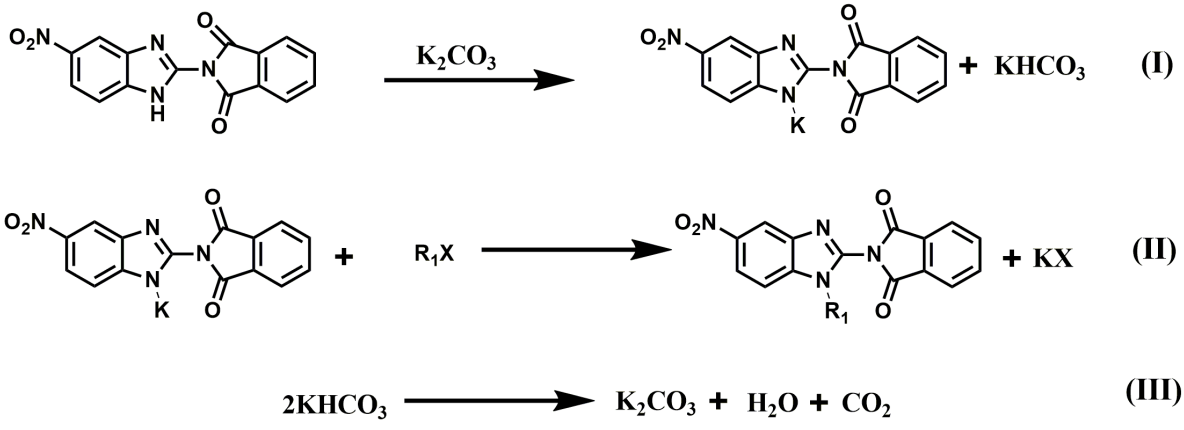

Table 1. *In vitro* cycloxygenases, lipoxygenases and TNF-α inhibition data for compounds (**3a-l).**

Target compound	COX-1 (IC_{50}[a]±SD[b],µM)	COX-2 (IC_{50}[a]±SD[b],µM)	Selectivity index (SI)[d]	5-LOX (IC_{50}[a]±SD[b],µM)	15-LOX (IC_{50}[a]±SD[b],µM)	TNF-α (IC_{50}[a]±SD[b],µM)
3a	23.73±0.05	23.00±0.04	1.03	2.44±0.17	3.64±0.34	>500
3b	52.66±0.20	354.6±1.34	0.14	3.36±0.207	7.74±0.26	>500
3c	7.76±0.10	181.8±0.98	0.04	7.30±0.08	5.93±0.03	>500
3d	8.56±0.03	2.08±0.05	4.11	4.37±0.02	6.98±0.12	>500
3e	41.15±0.70	44.24±1.11	0.93	3.06±0.02	9.38±0.19	n.a.
3f	452.50±0.84	29.73±0.19	15.2	5.04±0.17	4.84±0.20	n.a.
3g	146.55±0.17	28.87±0.10	5.07	6.12±0.11	1.76±0.07	n.a.
3h	17.73±0.50	345.95±0.21	0.05	3.50±0.35	1.05±0.06	>500
3i	15.99±0.14	16.07±0.02	0.10	8.42±0.23	6.02±0.05	>500
3j	9.85±0.03	1.00±0.02	9.85	0.32±0.07[#]	1.02±0.03	461.2±0.14
3k	28.87±0.04	372.0±0.91	0.07	5.66±0.07	7.40±0.20	>500
3l	8.80±0.04	27.48±0.07	0.32	4.83±0.09	9.48±0.17	>500
Indomethacin[c]	0.35±0.02	4.12±0.10	0.08	----	----	----
Celecoxib[c]	15.30±0.26	0.044±0.02	348	----	----	----
NDGA[c]	----	----	----	0.52±0.24	1.10±0.04	----
Dexamethasone[c]	----	----	----	----	----	11.04±0.05

[a] IC_{50} values represent the half maximal (50%) inhibitory concentration.
[b] Data are expressed as mean±SD (n=2). Data were statistically analysed by one way ANOVA followed by Tukey's post hoc test.
*P<0.05 vs. Std; #No statistical difference was found.
[c] Reference standards used for the present study.
[d] In vitro COX-2 selectivity index (COX-1/COX-2 IC_{50})
n.a, not active even at higher tested concentration.

Table 2 Anti-inflammatory data of the 2-(1-([1,1'-Biphenyl]-3-ylmethyl)-5-nitro-1*H*-benzo[d]imidazol-2-yl)isoindoline-1,3-dione (**3j**) on carrageenan-induced paw edema in rats.

Treatment	**Volume of paw edema (mL)***	
	3h	5h
Normal control (Untreated)	---	---
Control(Carrageenan treated)	14.8±0.75	15.5±0.83
Indomethacin(reference standard)[a,#]	3.16±0.63(79.41±4.91)[b]	7.50±0.54(51.46±4.67)[c]
Celecoxib(reference standard)[a,#]	1.83±0.44(87.59±3.09)	6.83±0.40(55.36±3.16)
3j[a]	2.66±0.81(81.88±6.08)	7.33±0.81(52.57±5.82)

*Data shown as mean±SD (n=6 rats per group). Data was analysed by Two way ANOVA followed by pairwise comparison using Bonferroni post hoc test.
Values in parenthesis (percentage inhibition of edema)
[a]P<0.001 vs carrageenan control group; [b]P<0.05 vs celecoxib; [c]No statistical difference was found vs celecoxib; [#]No statistical difference was found vs 3j.

Table 3. Analgesic, ulcerogenic and lipid peroxidation activities of the compound **3j**

Compounds	Analgesic activity[a] Mean writhes±SD at 3hr(%inhibition)	Ulcerogenic activity[b] Severity index±SD	Lipid peroxidation assay[c] nmol MDA content±SD/100mg tissue
Control	7.00±0.63	0.50±0.00	1.09±0.07
3j	1.66±0.51(76.28) ***	1.16±1.04[#,^]	1.17±0.08[d,e]
Indomethacin	1.50±0.83(78.57) ***	5.33±0.47 [*]	2.89±0.05[f]
Celecoxib	1.33±0.52(81.00) ***	0.66±0.57[*]	1.12±0.10[g]

[a] Inhibitory activity in the rat 4% NaCl-induced writhing assay at 3hr post drug administration. Percentage inhibition of writhing responses shown in parenthesis. Data are shown as the mean ± SD (n = 6 rats per group). ***P < 0.001 vs vehicle control group; one-way ANOVA followed by Tukey's post hoc test.

[b] The mean gastric lesion scores of each treated group minus the mean gastric lesion scores of the control group was considered as the "severity index" of gastric mucosa. Data are shown as the mean ± SD (n = 3 rats per group).[*]P<0.05 vs vehicle control group; [#]P<0.05 vs indomethacin *per se* treatment; [^]P<0.05 vs celecoxib *per se* treatment; Kruskal-Wallis followed by Mann-Whitney Test.

[c] Measurement of lipid peroxides in rat gastric mucosa demonstrated disruption of gastric membrane integrity. Data are shown as the mean ± SD (n = 3 rats per group).[d]P<0.05 vs vehicle control group, no statistical difference was found; [e]P<0.001 vs indomethacin *per se* treatment; [f]P<0.001 vs vehicle control group; [g]P<0.001 vs vehicle control group; one-way ANOVA followed by Tukey's post hoc test.

Highlights

- Benzimidazole scaffold based hybrids represents promising multitargeting potential by influencing various inflammation-related targets such as COX-1, COX-2, 5-LOX, 15-LOX and TNF-α.
- The most potent compound was further subjected to *in vivo* anti-inflammatory screening in conjunction with analgesic, ulcerogenic and lipid peroxidation activities.
- Additionally, active compound further exposed to molecular docking studies to deduce out binding mode with target proteins.

Graphical abstract